

*Supporting Information*

**Single crystal to single crystal transformation of spin-crossover coordination polymers from 3D frameworks to 2D layers**

Yu Gong,<sup>‡a</sup> Wang-Kang Han,<sup>‡a</sup> Hui-Shu Lu,<sup>a</sup> Qing-Tao Hu,<sup>a</sup> Huan Tu,<sup>a</sup> Pei-Ni Li,<sup>a</sup> Xiaodong Yan,<sup>a</sup> and Zhi-Guo Gu<sup>\*ab</sup>

<sup>a</sup> Key Laboratory of Synthetic and Biological Colloids, Ministry of Education, School of Chemical and Material Engineering, Jiangnan University, Wuxi 214122, China

<sup>b</sup> International Joint Research Center for Photoresponsive Molecules and Materials, School of Chemical and Material Engineering, Jiangnan University, Wuxi 214122, China

E-mail: [zhiguogu@jiangnan.edu.cn](mailto:zhiguogu@jiangnan.edu.cn)

## **1. Materials and physical measurements**

$\text{Fe}(\text{BF}_4)_2 \cdot 6\text{H}_2\text{O}$ , pyrazinamide, 2-methoxypyrazine, ethylpyrazine,  $\text{K}_2[\text{Pt}(\text{CN})_4] \cdot 3\text{H}_2\text{O}$ ,  $\text{K}_2[\text{Pd}(\text{CN})_4] \cdot 3\text{H}_2\text{O}$ , ascorbic acid and ethanol were all reagent grade and purchased from Sigma-Aldrich and used without further purification. Ultrapure milli-Q water ( $18.2 \text{ M}\Omega \cdot \text{cm}$ ) was used in all experiments.

In order to eliminate the effect of solvent molecules on the results, all tests were performed on desolvated samples of MOFs. The samples were dried in vacuum at  $60^\circ\text{C}$  for 24 hours for desolvation. The Fourier transform infrared (FT-IR) spectra were recorded by FALAN2000 FT-IR spectrometer (ABB Bomen Canada) (KBr disk). Element analyses were conducted on elementar corporation vario EL III analyzer. Raman spectra were obtained from Invia Raman spectre (Reinshaw England) with 785 nm excitation line. The laser power intensity was adjusted by changing the percentage of 280 mW, the largest laser power intensity in 785 nm excitation line. Powder X-ray diffraction (PXRD) patterns were collected on a D8 Advance X-ray diffractometer (Bruker AXS Germany) with Cu K $\alpha$  radiation in a  $2\theta$  range from  $5^\circ$  to  $60^\circ$  at the speed of  $2^\circ \text{ min}^{-1}$ . Variable-temperature magnetic susceptibilities on crystalline samples were performed on a Quantum Design MPMS-XL-7 SQUID magnetometer with an applied magnetic field of 1000 Oe over two temperature ranges of 3 K to 350 K in warming mode and 350 K to 3 K in cooling mode with sweep rate of  $3 \text{ K} \cdot \text{min}^{-1}$ . The molar susceptibilities were corrected for diamagnetic contributions using Pascal's constants and the increment method.

## 2. Synthesis and characterization

### 2.1 Synthesis and characterization of **1a** crystals

In a 15 mL test tube, 8 mL mixture solution of ethanol and H<sub>2</sub>O (v/v, 1:1) was slowly layered on the top of a 2 mL water solution of K<sub>2</sub>[Pd(CN)<sub>4</sub>]·3H<sub>2</sub>O (13.72 mg, 0.04 mmol). Then, 2 mL ethanol solution of ethylpyrazine (17.3 mg, 0.16 mmol) and Fe(BF<sub>4</sub>)<sub>2</sub>·6H<sub>2</sub>O (10.1 mg, 0.04 mmol) was carefully dropped as the third layer under room temperature, cubic shaped orange crystals were obtained after 2 weeks. Yield: 35%. Anal. Calcd for C<sub>10</sub>H<sub>8</sub>FeN<sub>6</sub>Pd: C, 32.07; H, 2.15; N, 22.45. Found: C, 32.11; H, 2.13; N, 22.46. IR (KBr,  $\nu$  cm<sup>-1</sup>, Fig. S1): 3421, 2358, 2171, 1624, 1405, 1162, 1085, 1041, 839.

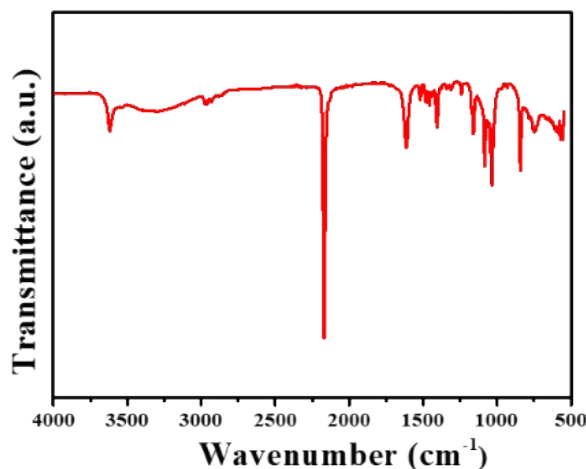


**Fig. S1** FT-IR spectrum of **1a**.

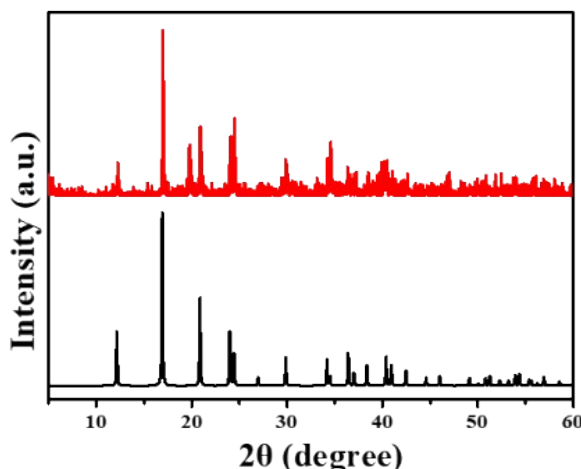


**Fig. S2** Comparison of the experimental PXRD pattern of simulated **1a** (black line) with as-prepared **1a** diffraction pattern (red line).

## 2.2 Synthesis and characterization of **1b** crystals

Single crystals of **1b** were synthesized using the procedure described for **1a**, substituting  $K_2[Pt(CN)_4] \cdot 3H_2O$  (17.24 mg, 0.04 mmol) for  $K_2[Pd(CN)_4] \cdot 3H_2O$  (13.72 mg, 0.04 mmol). Yield: 38%. Anal. Calcd for  $C_{10}H_8PtN_6Fe$ : C, 25.93; H, 1.74; N, 18.15. Found: C, 25.92; H, 1.73; N, 18.16. IR (KBr,  $\text{cm}^{-1}$ , Fig. S4): 3421, 2358, 2171, 1624, 1405, 1162, 1085, 1041.

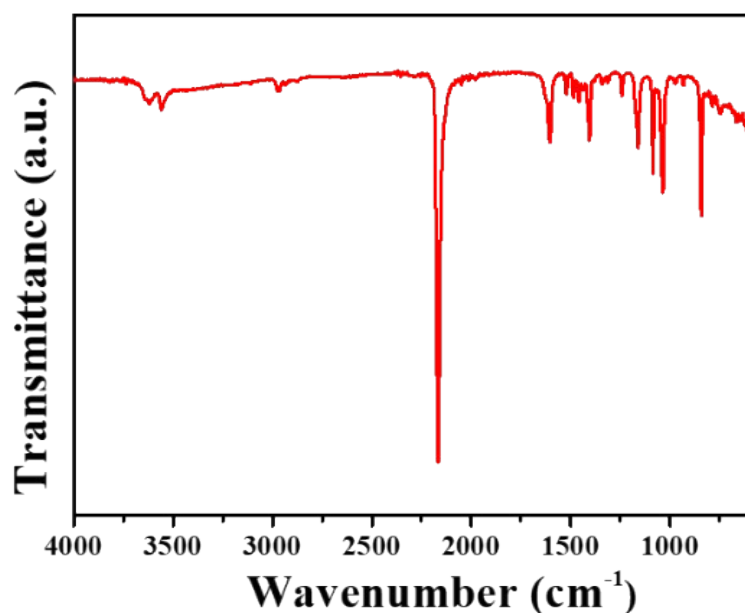


**Fig. S3** FT-IR spectrum of **1b**.

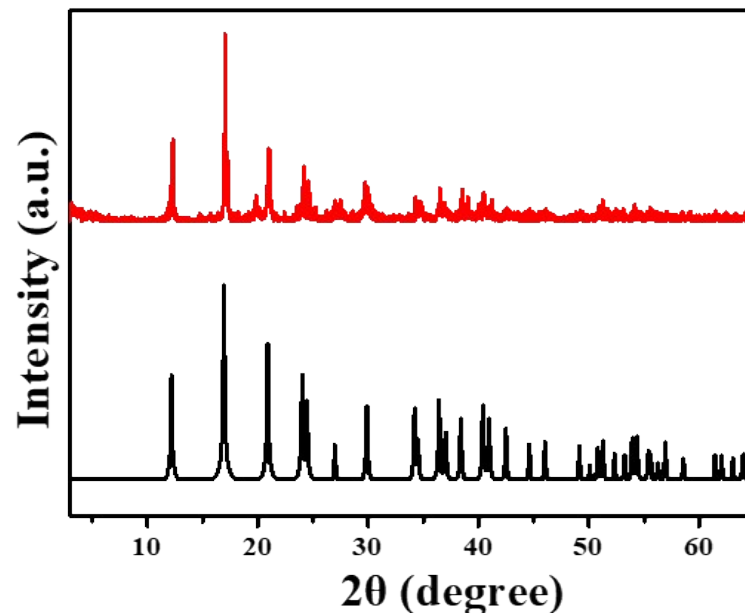


**Fig. S4** Comparison of the experimental PXRD pattern of simulated **1b** (black line) with as-prepared **1b** diffraction pattern (red line).

### 2.3 Synthesis and characterization of 2a crystals

The crystals **2a** were obtained in a same way by replacing the pillared-ligands in ethanol with 2-methoxypyrazine (11.8 mg, 0.16 mmol). Yield: 42%. Anal. Calcd for C<sub>14</sub>H<sub>12</sub>FeN<sub>8</sub>O<sub>2</sub>Pd: C, 34.56; H, 2.49; N, 23.03. Found: C, 34.52; H, 2.43; N, 23.06. IR (KBr, vcm<sup>-1</sup>, Fig. S7): 3441, 2162, 1599, 1399, 1540, 1402, 1328, 1197, 1138, 1065, 1003, 913, 838.

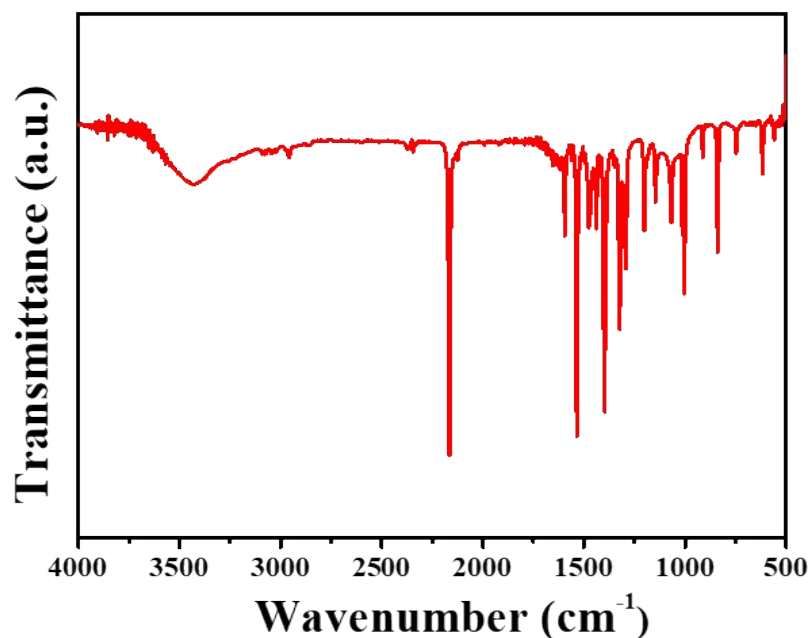


**Fig. S5** FT-IR spectrum of **2a**.

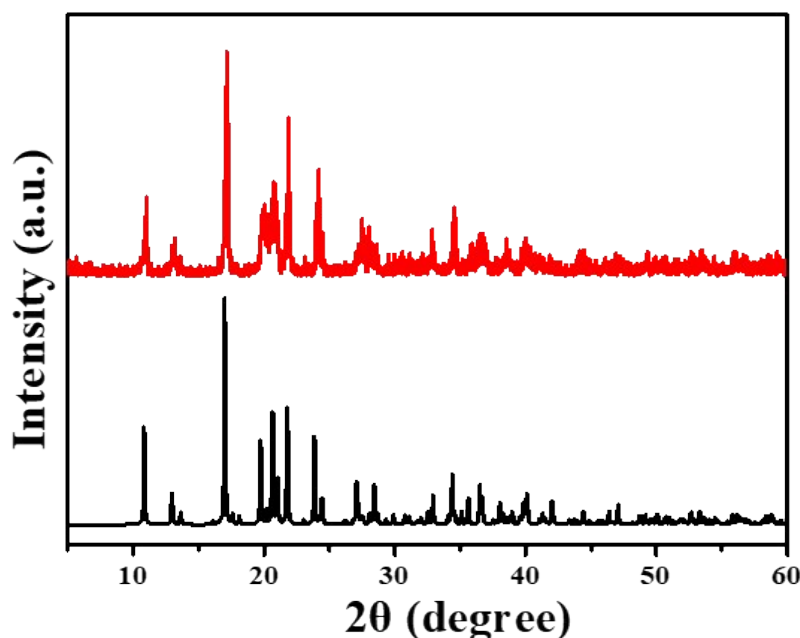


**Fig. S6** Comparison of the experimental PXRD pattern of simulated **2a** (black line) with as-prepared **2a** diffraction pattern (red line).

## 2.4 Synthesis and characterization of **2b** crystals

Single crystals of **2b** were synthesized using the procedure described for **2a**, substituting  $K_2[Pd(CN)_4] \cdot 3H_2O$  (13.72 mg, 0.04 mmol) for  $K_2[Pt(CN)_4] \cdot 3H_2O$  (17.24 mg, 0.04 mmol). Yield: 38%. Anal. Calcd for  $C_{14}H_{12}PtN_8O_2Fe$ : C, 29.23; H, 2.10; N, 19.48. Found: C, 29.22; H, 2.13; N, 19.46. IR (KBr,  $\text{cm}^{-1}$ , Fig. S10): 3431, 2164, 1578, 1526, 1399, 1329, 1292, 1197, 1138, 1073, 1000, 832, 612.

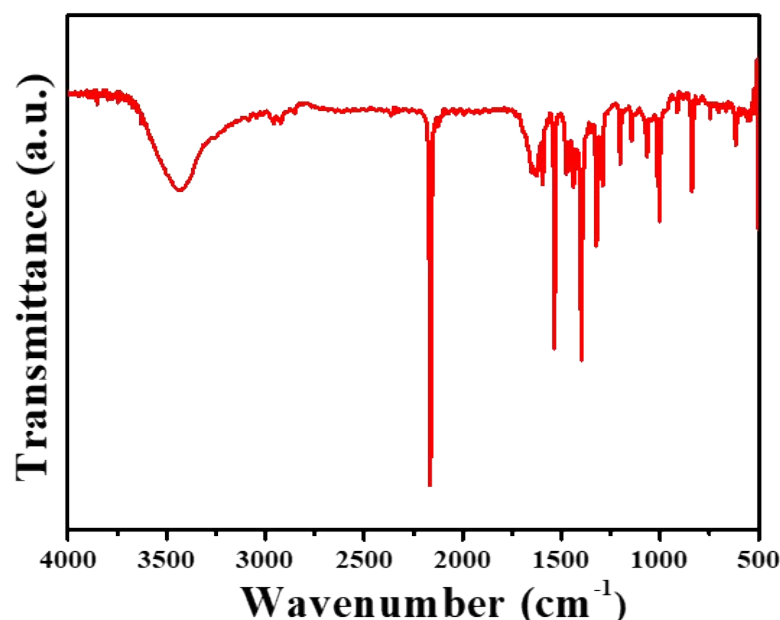


**Fig. S7** FT-IR spectrum of **2b**.

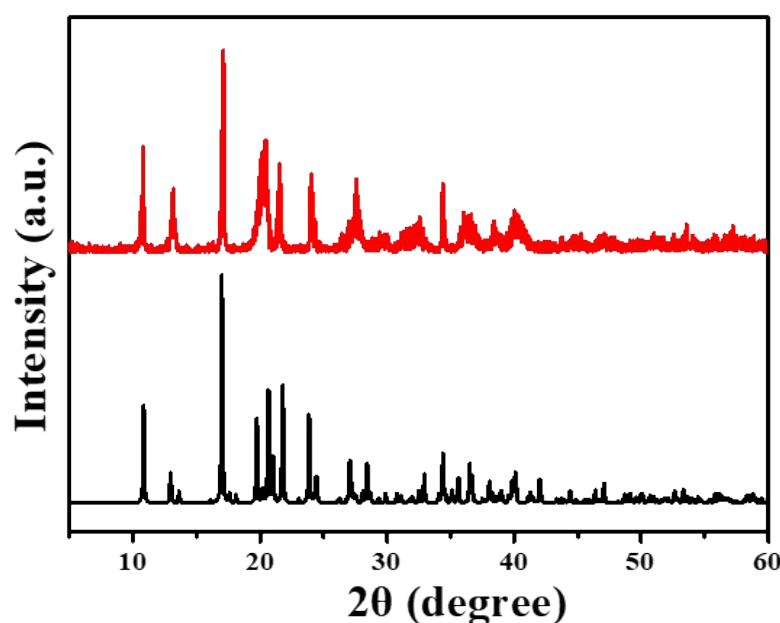


**Fig. S8** Comparison of the experimental PXRD pattern of simulated **2b** (black line) with as-prepared **2b** diffraction pattern (red line).

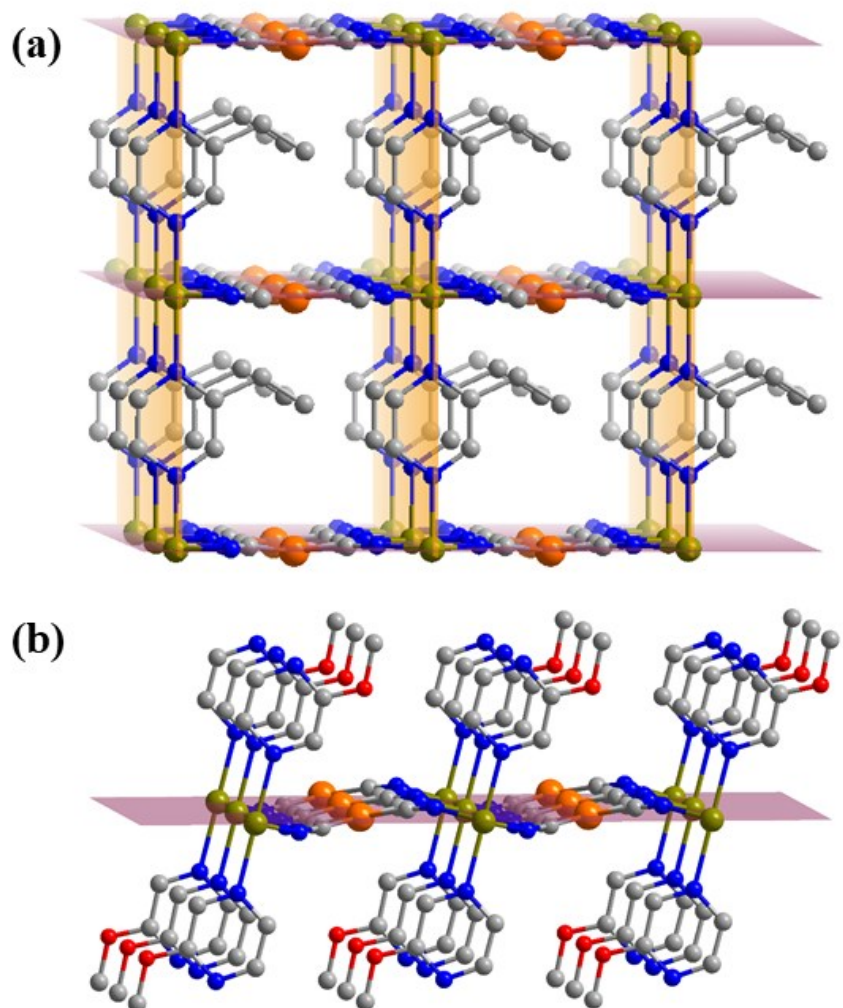


**Fig. S9** Crystal structures: (a) **1a**, (b) **2a**, (Pd: orange; Fe: yellow; C: gray; N: blue; O: red). All H atoms have been omitted for clarity.

## 2.5 The thermal stability of 1a, 1b, 2a and 2b

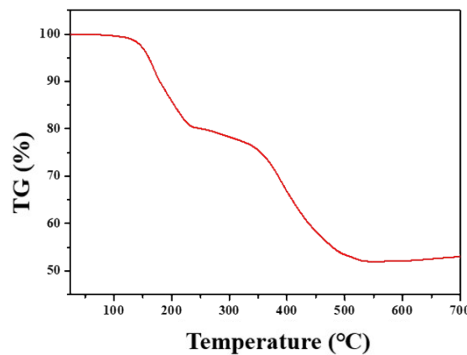


**Fig. S10** TG curve of 1a.

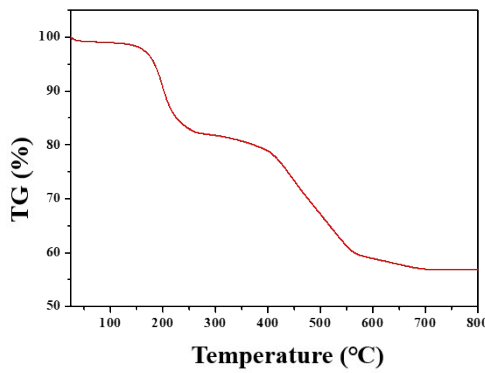


**Fig. S11** TG curve of 1b.

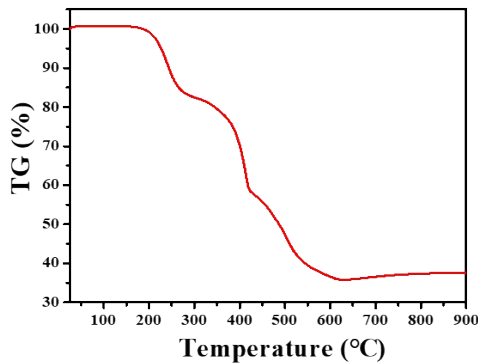


**Fig. S12** TG curve of 2a.

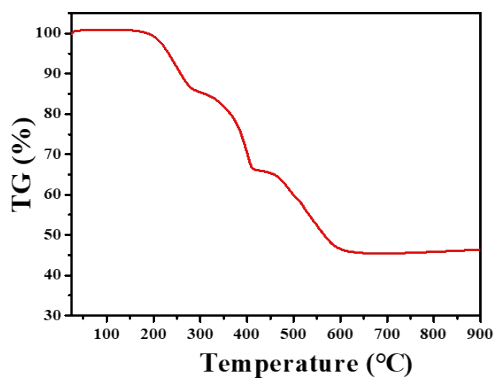


**Fig. S13** TG curve of 2b.

## 2.6 Characterization of SCSC transformation for **1b** crystals

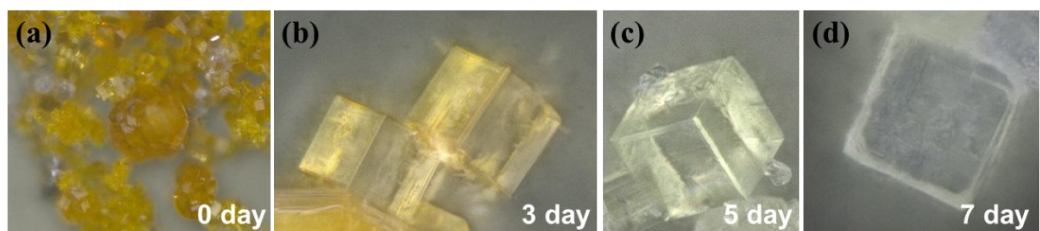


**Fig. S14** The optical microscopic photographs of colour change for **1b** before and after induced conversion by soaking in the solution of methoxypyrazine.

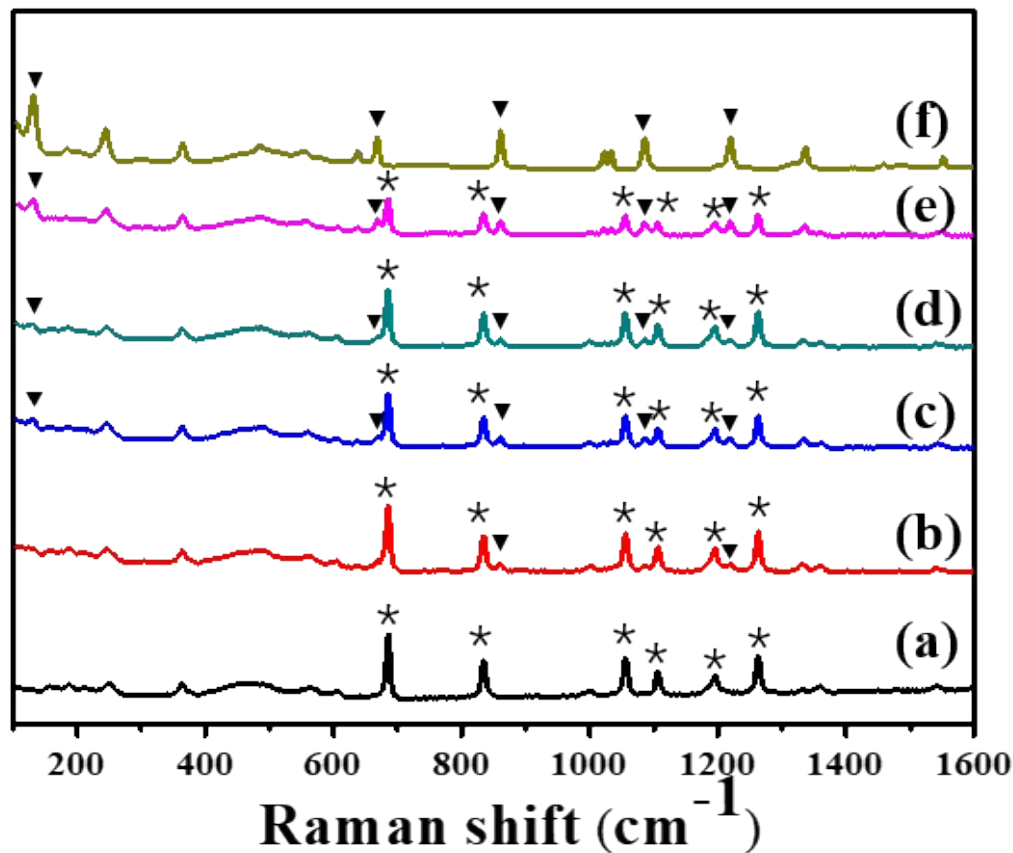


**Fig. S15** The change process as shown by Raman patterns for **1b** before and after induced conversion by soaking in the solution of methoxypyrazine (a) 0 day; (b) after 2 days; (c) after 3 days; (d) after 4 days; (e) after 5 days; (f) after 7 days.

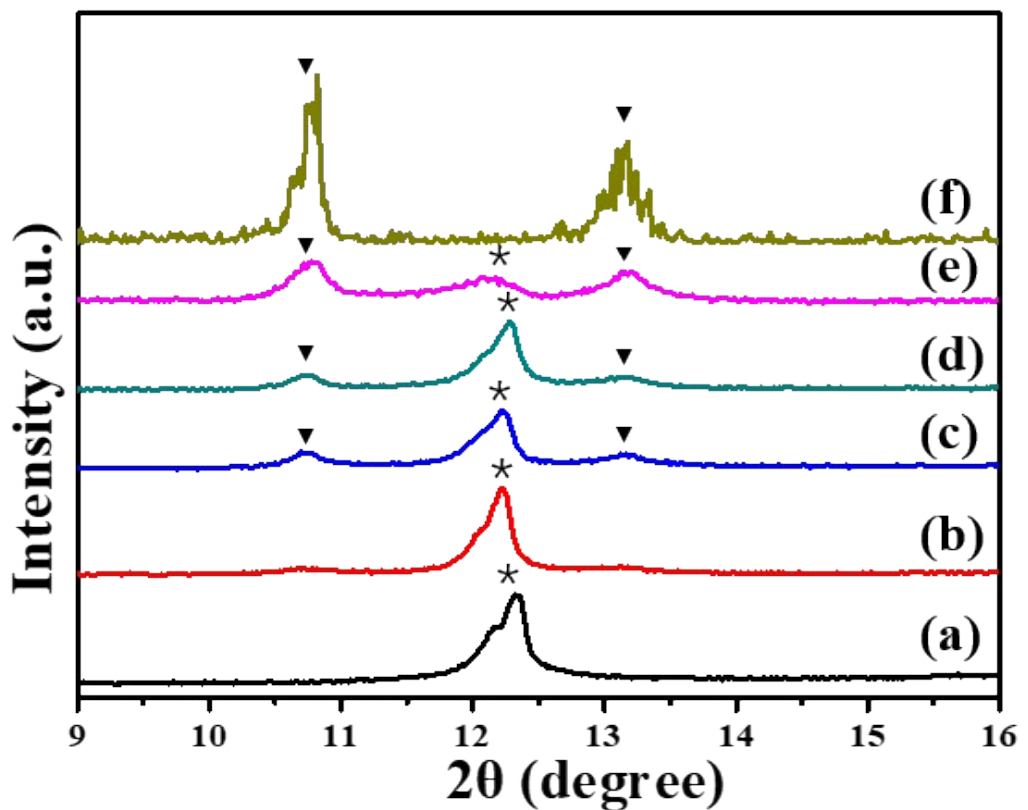


**Fig. S16** The change process as shown by PXRD patterns for **1b** before and after induced conversion by soaking in the solution of methoxypyrazine (a) 0 day; (b) after 2 days; (c) after 3 days; (d) after 4 days; (e) after 5 days; (f) after 7 days.

### 3. X-ray crystallography

The crystal structures were determined on a Siemens (Bruker) SMART CCD diffractometer using monochromated Mo  $K\alpha$  radiation ( $\lambda = 0.71073 \text{ \AA}$ ) at 173 K. Cell parameters were retrieved using SMART software and refined using SAINT<sup>[4]</sup> on all observed reflections. The highly redundant data sets were reduced using SAINT<sup>[4]</sup> and corrected for Lorentz and polarization effects. Absorption corrections were applied using SADABS<sup>[5]</sup> supplied by Bruker. Structures were solved by direct methods using the program SHELXL-2014-7.<sup>[6]</sup> All of the non-hydrogen atoms were refined with anisotropic thermal displacement coefficients. Hydrogen atoms of organic ligands were located geometrically and refined in a riding model, whereas those of solvent molecules were not treated during the structural refinements. Disorder was modeled using standard crystallographic methods including constraints, restraints and rigid bodies where necessary. The crystals of **1a** and **1b** are very small, despite crystal quality was very good, the data collected were less than ideal quality. Disorder was modeled using standard crystallographic methods including constraints, restraints and rigid bodies where necessary. Reflecting the instability of the crystals, there were a large area of smeared electron density present in the lattice. Despite many attempts to model this region of disorder as a combination of solvent molecules no reasonable fit could be found and accordingly these regions were treated with the SQUEEZE function of PLATON. For **1a**, ethylpyrazine groups are disordered. For **1b**, ethylpyrazine groups are disordered. Final crystallographic data for **1a**, **1b**, **2a** and **2b** are listed in Table S1-S4, and the selected bond distances [ $\text{\AA}$ ] and angles [°] are listed in Table S5-S8.

**Table S1** Summary of crystallographic data for **1a** at different temperatures.

[Fe(ep)Pd(CN) <sub>4</sub> ]					
Temp / K	80 K	130 K	173 K	196 K	273 K
Formula	C <sub>10</sub> H <sub>8</sub> FeN <sub>6</sub> Pd	C <sub>10</sub> H <sub>8</sub> FeN <sub>6</sub> Pd	C <sub>5</sub> H <sub>4</sub> Fe <sub>0.50</sub> N <sub>3</sub> Pd <sub>0.50</sub>	C <sub>10</sub> H <sub>8</sub> FeN <sub>6</sub> Pd	C <sub>10</sub> H <sub>8</sub> FeN <sub>6</sub> Pd
Fw	374.47	374.47	187.2	374.47	374.47
cryst syst	tetragonal	tetragonal	tetragonal	tetragonal	tetragonal
space group	<i>P</i> 4/ <i>mmm</i>	<i>P</i> 4/ <i>mmm</i>	<i>P</i> 4/ <i>mmm</i>	<i>P</i> 4/ <i>mmm</i>	<i>P</i> 4/ <i>mmm</i>
<i>a</i> , Å	7.3924(2)	7.4015(2)	5.2430(4)	7.4182(2)	7.4410(11)
<i>b</i> , Å	7.3924(2)	7.4015(2)	5.2430(4)	7.4182(2)	7.4410(11)
<i>c</i> , Å	7.2295(4)	7.2608(5)	7.2830(11)	7.2986(4)	7.3392(19)
$\alpha$ deg	90	90	90	90	90
$\beta$ deg	90	90	90	90	90
$\gamma$ deg	90	90	90	90	90
Z	1	1	1	1	1
V, Å <sup>3</sup>	395.07(3)	397.76(4)	200.20(4)	401.64(3)	406.36(16)
Calcd, g cm <sup>-3</sup>	1.574	1.563	1.553	1.548	1.530
T (K)	80(2)	130(2)	173(2)	195(2)	273(2)
$\lambda$ (Å)	1.34139	1.34139	0.71073	1.34139	1.34139
F(000)	182	182	91	182	182
$\theta$ range (deg)	5.32 ~ 59.40 -8 ≤ h ≤ 9, -9 ≤ k ≤ 9, -9 ≤ l ≤ 9	7.43 ~ 56.47 -9 ≤ h ≤ 4, -8 ≤ k ≤ 9, -9 ≤ l ≤ 9	4.8 ~ 25.1 -6 ≤ h ≤ 5, -6 ≤ k ≤ 6, -7 ≤ l ≤ 8	7.41 ~ 58.63 -9 ≤ h ≤ 6, -8 ≤ k ≤ 9, -9 ≤ l ≤ 7	7.37 ~ 58.38 -9 ≤ h ≤ 8, -9 ≤ k ≤ 9, -9 ≤ l ≤ 9
Index ranges					
GOF on F <sup>2</sup>	0.997	1.164	1.026	1.063	1.152
Reflections collected	299	301	136	317	314
R <sub>I</sub> <sup>a</sup> , wR <sub>2</sub> <sup>b</sup> (I>2σ(I))	0.0418, 0.1117	0.0582, 0.1579	0.0401, 0.0979	0.0500, 0.1411	0.0597, 0.1609
R <sub>I</sub> <sup>a</sup> , wR <sub>2</sub> <sup>b</sup> (all data)	0.0418, 0.1119	0.0616, 0.1633	0.0406, 0.0981	0.0525, 0.1456	0.0636, 0.1657

$$R_I^a = \Sigma ||F_o| - |F_c||/\Sigma F_o|. \quad wR_2^b = [\Sigma w(F_o^2 - F_c^2)^2/\Sigma w(F_o^2)]^{1/2}$$

**Table S2** Summary of crystallographic data for **1b** at different temperatures.

[Fe(ep)Pt(CN) <sub>4</sub> ]					
Temp / K	80 K	120 K	173 K	246 K	273 K
Formula	C <sub>10</sub> H <sub>8</sub> FeN <sub>6</sub> Pt				
Fw	463.16	463.16	463.16	463.16	463.16
cryst syst	tetragonal	tetragonal	tetragonal	tetragonal	tetragonal
space group	<i>P4/mmm</i>	<i>P4/mmm</i>	<i>Pm2</i>	<i>P4/mmm</i>	<i>P4/mmm</i>
<i>a</i> , Å	7.3990(6)	7.4028(6)	7.4055(9)	7.4300(6)	7.4379(9)
<i>b</i> , Å	7.3990(6)	7.4028(6)	7.4055(9)	7.4300(6)	7.4379(9)
<i>c</i> , Å	7.2470(10)	7.2640(10)	7.2816(15)	7.3437(10)	7.3721(16)
$\alpha$ deg	90	90	90	90	90
$\beta$ deg	90	90	90	90	90
$\gamma$ deg	90	90	90	90	90
Z	1	1	1	1	1
V, Å <sup>3</sup>	396.74(8)	398.08(8)	399.33(13)	405.41(8)	407.84(13)
Calcd, g cm <sup>-3</sup>	1.939	1.932	1.926	1.897	1.886
T (K)	80(2)	120(2)	173(2)	273(2)	273(2)
$\lambda$ (Å)	1.34139	1.34139	0.71073	1.34139	1.34139
F(000)	214	214	214	214	214
$\theta$ range (deg)	5.20 ~ 63.04 -8 ≤ h ≤ 9,	5.20 ~ 63.73 -9 ≤ h ≤ 9,	3.9 ~ 25.4 -8 ≤ h ≤ 8,	5.18 ~ 62.40 -9 ≤ h ≤ 9,	5.17 ~ 62.23 -9 ≤ h ≤ 9,
Index ranges	-8 ≤ k ≤ 9, -9 ≤ l ≤ 9	-9 ≤ k ≤ 9, -9 ≤ l ≤ 9	-8 ≤ k ≤ 8, -8 ≤ l ≤ 8	-7 ≤ k ≤ 9, -9 ≤ l ≤ 9	-7 ≤ k ≤ 9, -9 ≤ l ≤ 9
GOF on F <sup>2</sup>	1.114	1.020	1.041	1.173	1.052
Reflections collected	327	327	389	327	332
R <sub>I</sub> <sup>a</sup> , wR <sub>2</sub> <sup>b</sup> (I>2σ(I))	0.0488, 0.1392	0.0664, 0.1625	0.0508, 0.1041	0.0559, 0.1511	0.0527, 0.1333
R <sub>I</sub> <sup>a</sup> , wR <sub>2</sub> <sup>b</sup> (all data)	0.0491, 0.1395	0.0668, 0.1628	0.0606, 0.1073	0.0587, 0.1576	0.0531, 0.1339

$$R_I^a = \Sigma ||F_o| - |F_c||/\Sigma F_o|. \quad wR_2^b = [\Sigma w(F_o^2 - F_c^2)^2/\Sigma w(F_o^2)]^{1/2}$$

**Table S3** Summary of crystallographic data for **2a** at different temperatures.

[Fe(mp) <sub>2</sub> Pd(CN) <sub>4</sub> ]				
Temp / K	100 K	173 K	186 K	273 K
Formula	C <sub>14</sub> H <sub>12</sub> FeN <sub>8</sub> O <sub>2</sub> Pd	C <sub>14</sub> H <sub>12</sub> FeN <sub>8</sub> O <sub>2</sub> Pd	C <sub>14</sub> H <sub>12</sub> FeN <sub>8</sub> O <sub>2</sub> Pd	C <sub>14</sub> H <sub>12</sub> FeN <sub>8</sub> O <sub>2</sub> Pd
Fw	486.57	486.57	486.57	486.57
cryst syst	triclinic	Monoclinic	Monoclinic	monoclinic
space group	<i>P</i> -1	<i>P</i> 2/n	<i>C</i> 2/m	<i>C</i> 2/m
<i>a</i> , Å	7.0822(10)	7.3053(7)	17.495(3)	17.639(2)
<i>b</i> , Å	7.2506(9)	7.4566(7)	7.4481(12)	7.4328(10)
<i>c</i> , Å	9.3076(13)	16.3514(16)	7.3114(10)	7.3645(9)
α deg	107.941(8)	90	90	90
β deg	111.972(8)	93.917(4)	110.996(13)	111.368(5)
γ deg	90.161(8)	90	90	90
Z	1	2	2	2
V, Å <sup>3</sup>	417.89(10)	888.62(15)	889.5(2)	899.2(2)
Calcd, g cm <sup>-3</sup>	1.933	1.819	1.817	1.797
T (K)	100(2)	173	186(2)	273(2)
λ (Å)	1.34139	0.71073	1.34139	1.34139
F(000)	240	480	480	480
θ range (deg)	4.73 ~ 59.40 -22 ≤ h ≤ 22,	3.0 ~ 25.4 - 8 ≤ h ≤ 8,	4.71 ~ 55.25 -6 ≤ h ≤ 21,	4.684 ~ 62.671 -9 ≤ h ≤ 8,
Index ranges	-9 ≤ k ≤ 8, 0 ≤ l ≤ 11	- 8 ≤ k ≤ 8, - 18 ≤ l ≤ 19	-8 ≤ k ≤ 9, -8 ≤ l ≤ 8	-9 ≤ k ≤ 9, 0 ≤ l ≤ 12
GOF on F <sup>2</sup>	1.067	1.043	1.131	1.191
Reflections collected	1107	1547	702	1041
R <sub>I</sub> <sup>a</sup> , wR <sub>2</sub> <sup>b</sup> (I>2σ(I))	0.0875, 0.2092	0.0477, 0.0958	0.0820, 0.2207	0.0639, 0.1843
R <sub>I</sub> <sup>a</sup> , wR <sub>2</sub> <sup>b</sup> (all data)	0.1145, 0.2259	0.0595, 0.1028	0.1021, 0.2300	0.0694, 0.1918

$$R_I^a = \Sigma ||F_o| - |F_c||/\Sigma F_o|. \quad wR_2^b = [\Sigma w(F_o^2 - F_c^2)^2/\Sigma w(F_o^2)]^{1/2}$$

**Table S4** Summary of crystallographic data for **2b** at different temperatures.

[Fe(mp) <sub>2</sub> Pt(CN) <sub>4</sub> ]				
Temp / K	100 K	173 K	194 K	273 K
Formula	C <sub>14</sub> H <sub>12</sub> FeN <sub>8</sub> O <sub>2</sub> Pt	C <sub>14</sub> H <sub>12</sub> FeN <sub>8</sub> O <sub>2</sub> Pt	C <sub>14</sub> H <sub>12</sub> FeN <sub>8</sub> O <sub>2</sub> Pt	C <sub>14</sub> H <sub>12</sub> FeN <sub>8</sub> O <sub>2</sub> Pt
Fw	575.26	575.26	575.26	575.26
cryst syst	Monoclinic	Monoclinic	Monoclinic	triclinic
space group	<i>C2/m</i>	<i>P</i>	<i>C2/m</i>	<i>P-1</i>
<i>a</i> , Å	17.8746(14)	7.0000(7)	17.9261(10)	7.3434(7)
<i>b</i> , Å	7.2176(5)	7.4565(7)	7.2278(4)	7.4514(6)
<i>c</i> , Å	7.1174(5)	9.3174(9)	7.1077(4)	9.5468(9)
$\alpha$ deg	90	108.903(3)	90	110.260(3)
$\beta$ deg	108.185(4)	110.402(3)	108.139(3)	110.977(3)
$\gamma$ deg	90	90.178(3)	90	90.082(3)
Z	2	1	2	1
V, Å <sup>3</sup>	872.37(11)	427.53(7)	875.15(9)	452.87(7)
Calcd, g cm <sup>-3</sup>	2.190	2.234	2.183	2.109
T (K)	100(2)	173	94(2)	273(2)
$\lambda$ (Å)	1.34139	0.71073	1.34139	1.34139
F(000)	544	272	544	272
$\theta$ range (deg)	2.79 ~ 24.61 -22 ≤ h ≤ 22,	2.9 ~ 26.0 -8 ≤ h ≤ 8,	4.516 ~ 62.731 -22 ≤ h ≤ 23,	5.563 ~ 63.144 -9 ≤ h ≤ 8,
Index ranges	-8 ≤ k ≤ 8, -8 ≤ l ≤ 8	-9 ≤ k ≤ 8, 0 ≤ l ≤ 11	-9 ≤ k ≤ 9, -9 ≤ l ≤ 9	-9 ≤ k ≤ 9, 0 ≤ l ≤ 12
GOF on F <sup>2</sup>	1.064	1.0	1.050	1.079
Reflections collected	854	1131	992	2074
$R_I^a, wR_2^b (I > 2\sigma(I))$	0.0329, 0.0877	0.0392, 0.0541	0.0728, 0.1776	0.0329, 0.0877
$R_I^a, wR_2^b (\text{all data})$	0.0329, 0.0877	0.0758, 0.0608	0.0859, 0.1910	0.0329, 0.0877

$$R_I^a = \Sigma |F_o| - |F_c| / \Sigma |F_o|. \quad wR_2^b = [\sum w(F_o^2 - F_c^2)^2 / \sum w(F_o^2)]^{1/2}$$

**Table S5** The main bond lengths (Å) and angles (°) of **1a**.

80 K			
Fe1–N1	2.093(6)	Fe1–N1h	2.093(6)
Fe1–N2	2.01(2)	Fe1–N2h	2.01(2)
Fe1–N3a	2.47(2)	Fe1–N3k	2.47(2)
Fe1–N3d	2.47(2)	Fe1–N1	2.093(6)
Fe1–N1e	2.093(6)	Fe1–N2	2.01(2)
Fe1–N2e	2.01(2)	Fe1–N3g	2.47(2)
N1–Fe1–N2	87.2(11)	N1–Fe1–N1e	90.0(2)
N1–Fe1–N2e	91.9(11)	N1–Fe1–N1h	180.00
N1–Fe1–N2h	92.8(11)	N1–Fe1–N1l	90.0(2)
N1–Fe1–N2l	88.1(11)	N1e–Fe1–N2	88.1(11)
N1h–Fe1–N2	92.8(11)	N1l–Fe1–N2	91.9(11)
N1e–Fe1–N1h	90.0(2)	N1e–Fe1–N2e	87.2(11)
N1e–Fe1–N2h	91.9(11)	N1e–Fe1–N1l	180.00
N1e–Fe1–N2l	92.8(11)	N1h–Fe1–N2e	88.1(11)
N1l–Fe1–N2e	92.8(11)		
130 K			
Fe1–N1	2.112(8)	Fe1–N1e	2.112(8)
Fe1–N2	2.03(3)	Fe1–N2e	2.03(3)
Fe1–N1h	2.112(8)	Fe1–N2h	2.03(3)
Fe1–N1l	2.112(8)	Fe1–N2l	2.03(3)
N1–Fe1–N2	88.4(11)	N1–Fe1–N1e	90.0(3)
N1–Fe1–N2e	93.4(11)	N1–Fe1–N1h	180.00
N1–Fe1–N2h	91.6(11)	N1–Fe1–N1l	90.0(3)
N1–Fe1–N2e	91.6(11)	N1e–Fe1–N2	86.6(11)
N2–Fe1–N2e	5.3(14)	N1h–Fe1–N2	91.6(11)
N1l–Fe1–N2	93.4(11)	N1e–Fe1–N2e	88.4(11)
N1e–Fe1–N1h	90.0(3)	N1e–Fe1–N2h	93.4(11)

N1e–Fe1–N1l	180.00	N1e–Fe1–N2l	91.6(11)
N1h–Fe1–N2e	86.6(11)		
<b>173 K</b>			
Fe(1)–N(1)	2(2)	Fe(1)–C(1)	2(2)
Fe(1)–N(1c)	2(2)	Fe(1)–N(1a)	2(2)
Fe(1)–N(1f)	2(2)	Fe(1)–N(2f)	2.2(7)
N1d–N1–N1f	73(2)	Fe(1)–N(1o)	2(2)
N2–Fe1–N2f	180.00	N1–Fe1–N1m	180.00
<b>195 K</b>			
Fe1–N1	2.134(7)	Fe1–N2	2.08(3)
Fe1–N1e	2.134(7)	Fe1–N2e	2.08(3)
Fe1–N1h	2.134(7)	Fe1–N2h	2.08(3)
Fe1–N1l	2.134(7)	Fe1–N2l	2.08(3)
N1–Fe1–N2	88.1(11)	N1–Fe1–N1e	90.0(3)
N1–Fe1–N2e	92.7(11)	N1–Fe1–N1h	180.00
N1–Fe1–N2h	91.9(11)	N1–Fe1–N1l	90.0(3)
N1–Fe1–N2l	87.3(11)	N1e–Fe1–N2	87.3(11)
N1h–Fe1–N2	91.9(11)	N1l–Fe1–N2	92.7(11)
N1e–Fe1–N2e	88.1(11)	N1e–Fe1–N1h	90.0(3)
<b>273 K</b>			
Fe1–N1	2.155(8)	Fe1–N2	2.15(4)
Fe1–N1e	2.155(8)	Fe1–N1h	2.155(8)
Fe1–N2h	2.15(4)	Fe1–N1l	2.155(8)
Fe1–N2e	2.15(4)	Fe1–N2l	2.15(4)
N1–Fe1–N2	88.0(10)	N1–Fe1–N1e	90.0(3)
N1–Fe1–N2e	93.1(10)	N1–Fe1–N1h	180.00
N1–Fe1–N2h	92.0(10)	N1–Fe1–N1l	90.0(3)
N1–Fe1–N2l	86.9(10)	N1e–Fe1–N2	86.9(10)
N1h–Fe1–N2	92.0(10)	N1l–Fe1–N2	93.1(10)
N1e–Fe1–N2e	88.0(10)	N1e–Fe1–N1h	90.0(3)
N1e–Fe1–N2h	93.1(10)	N1e–Fe1–N1l	180.00
N1e–Fe1–N2l	92.0(10)	N1l–Fe1–N2e	92.0(10)

**Table S6** The main bond lengths ( $\text{\AA}$ ) and angles ( $^\circ$ ) of **1b**.

80 K			
Fe1–N1	2.106(11)	Fe1–N2	1.9974(3)
Fe1–N1e	2.106(11)	Fe1–N2e	1.9974(3)
Fe1–N1h	2.106(11)	Fe1–N2h	1.9974(3)
Fe1–N1l	2.106(11)	Fe1–N2l	1.9974(3)
N1–Fe1–N2	86.79(1)	N1–Fe1–N1e	90.0(4)
N1–Fe1–N2e	92.79(2)	N1–Fe1–N1h	180.00
N1–Fe1–N2h	93.22(1)	N1–Fe1–N1l	90.0(4)
N1–Fe1–N2l	87.21(2)	N1e–Fe1–N2	87.21(2)
N1h–Fe1–N2	93.22(1)	N1l–Fe1–N2	92.79(2)
N1e–Fe1–N1h	90.0(4)	N1e–Fe1–N2h	92.79(2)
N1e–Fe1–N1l	180.00	N1e–Fe1–N2l	93.22(1)
N1h–Fe1–N2e	87.21(2)	N1l–Fe1–N2e	93.22(1)
120 K			
Fe1–N1	2.114(13)	Fe1–N2	2.0020(3)
Fe1–N1e	2.114(13)	Fe1–N2e	2.0020(3)
Fe1–N1h	2.114(13)	Fe1–N2h	2.0020(3)
Fe1–N1l	2.114(13)	Fe1–N2l	2.0020(3)
N1–Fe1–N2	86.79(2)	N1–Fe1–N1e	90.0(5)
N1–Fe1–N2e	92.79(2)	N1–Fe1–N1h	180.00
N1–Fe1–N2h	93.21(2)	N1–Fe1–N1l	90.0(5)
N1–Fe1–N2l	87.21(2)	N1e–Fe1–N2	87.21(2)
N1h–Fe1–N2	93.21(2)	N1l–Fe1–N2	92.79(2)
N1e–Fe1–N2e	86.79(2)	N1e–Fe1–N1h	90.0(5)
N1e–Fe1–N2h	92.79(2)	N1e–Fe1–N1l	180.00
173 K			
Fe(1)–N(1)	2.106(15)	Fe(1)–N(2)	1.820(16)
Fe(1)–N(3b)	2.469(16)	N1g–Fe1–N3b	78.9(4)

N2–Fe1–N2g	180.00	N1g–Fe1–N2g	78.9(4)
N1–Fe1–N2	88.3(4)	N2–Fe1–N1g	101.1(4)
N1–Fe1–N3b	91.7(4)		
<b>246 K</b>			
Fe1–N1	2.129(13)	Fe1–N2	2.0239(3)
N1–Fe1–N2	86.81(2)	N1–Fe1–N2	86.81(2)
N1–Fe1–N2b	92.77(2)	N1–Fe1–N1c	180.00
N1–Fe1–N2c	93.19(2)	N1–Fe1–N2e	87.23(2)
N2–Fe1–N2h	171.58	N2–Fe1–N2i	174.47
N2–Fe1–N2k	179.41	N2–Fe1–N2m	173.63
<b>273 K</b>			
Fe1–N1	2.124(11)	Fe1–N2	2.0317(4)
N1–Fe1–N2	86.82(1)	N1–Fe1–N1b	90.0(4)
N1–Fe1–N2b	92.76(2)	N1–Fe1–N1c	180.00
N1–Fe1–N2c	93.18(1)	N1–Fe1–N2e	87.24(2)
N2–Fe1–N2h	171.60	N2–Fe1–N2i	174.48
N2–Fe1–N2k	179.41	N2–Fe1–N2m	173.65

**Table S7** The main bond lengths (Å) and angles (°) of **2a**.

100 K			
Fe1–N1	1.996(16)	Fe1–N4	1.95(2)
Fe1–N3a	1.94(2)	Fe1–N1c	1.996(16)
Fe1–N4c	1.95(2)	Fe1–N3d	1.94(2)
N1–Fe1–N4	89.2(9)	N1–Fe1–N3a	91.8(9)
N1–Fe1–N1c	180.00	N1–Fe1–N4c	90.8(9)
N1–Fe1–N3d	88.2(9)	N3a–Fe1–N4	89.9(10)
N1c–Fe1–N4	90.8(9)	N4–Fe1–N4c	180.00
N3d–Fe1–N4	90.1(10)	N1c–Fe1–N3a	88.2(9)
N3a–Fe1–N4c	90.1(10)	N3a–Fe1–N3d	180.00
N1c–Fe1–N4c	89.2(9)	N1c–Fe1–N3d	91.8(9)
N3d–Fe1–N4c	89.9(10)		
173 K			
Fe(1)–N(1)	2.132(4)	N1–Fe1–N4	91.33(17)
Fe(1)–N(4)	2.221(3)	N1–Fe1–N2a	179.20(18)
Fe(1)–N(2a)	2.138(4)	N1–Fe1–N1c	90.67(16)
Fe(1)–N(1c)	2.132(4)	N1–Fe1–N4c	88.65(17)
Fe(1)–N(4c)	2.221(3)	N1–Fe1–N2d	89.06(16)
Fe(1)–N(2d)	2.138(4)	N2a–Fe1–N4	87.91(17)
N1c–Fe1–N4	88.65(17)	N4–Fe1–N4c	180.00
N2d–Fe1–N4	92.11(17)	N1c–Fe1–N2a	89.06(16)
N2a–Fe1–N4c	92.11(17)	N2–Fe1–N2d	91.22(16)
N1c–Fe1–N4c	91.33(17)	N1c–Fe1–N2d	179.20(18)
N2d–Fe1–N4c	87.91(17)		
194 K			
Fe1–N1	1.996(18)	Fe1–N3	1.942(9)
Fe1–N1a	1.996(18)	Fe1–N3a	1.942(9)
Fe1–N3c	1.942(9)	Fe1–N3e	1.942(9)
N1–Fe1–N3	90.1(5)	N1–Fe1–N1a	180.00
N1–Fe1–N3a	89.9(5)	N1–Fe1–N3c	89.9(5)
N1–Fe1–N3e	90.1(5)	N1a–Fe1–N3	89.9(5)
N3–Fe1–N3a	89.9(4)	N3–Fe1–N3c	180.00
N3–Fe1–N3e	90.1(4)	N1a–Fe1–N3a	90.1(5)
N1a–Fe1–N3c	90.1(5)	N1a–Fe1–N3e	89.9(5)
N3a–Fe1–N3c	90.1(4)	N3a–Fe1–N3e	180.00
N3c–Fe1–N3e	89.9(4)		
273 K			
Fe1–N1	2.146(5)	Fe1–N1b	2.146(5)
Fe1–N2	2.231(7)	Fe1–N2b	2.231(7)
Fe1–N1d	2.146(5)	Fe1–N1	2.146(5)

N1–Fe1–N2	88.33(19)	N1b–Fe1–N2b	88.33(19)
N1–Fe1–N1b	91.38(18)	N1b–Fe1–N1d	88.62(18)
N1–Fe1–N2b	91.67(19)	N1b–Fe1–N1f	180.00
N1–Fe1–N1d	180.00	N1d–Fe1–N2b	88.33(19)
N1–Fe1–N1f	88.62(18)	N1f–Fe1–N2b	91.67(19)
N1b–Fe–N2	91.67(19)	N1d–Fe1–N1f	91.38(18)
N2–Fe1–N2b	180.00	N1f–Fe1–N2	88.33(19)
N1d–Fe1–N2	91.67(19)		

**Table S8** The main bond lengths ( $\text{\AA}$ ) and angles ( $^\circ$ ) of **2b**.

100 K			
Fe1–N1	2.00(2)	Fe1–N3	1.928(12)
Fe1–N1a	2.00(2)	Fe1–N3a	1.928(12)
Fe1–N3c	1.928(12)	Fe1–N3e	1.928(12)
N1–Fe1–N3	89.0(6)	N1–Fe1–N1a	180.00
N1–Fe1–N3a	91.0(6)	N1–Fe1–N3c	91.0(6)
N1–Fe1–N3e	89.0(6)	N1a–Fe1–N3	91.0(6)
N3–Fe1–N3a	90.7(5)	N3–Fe1–N3c	180.0
N3–Fe1–N3e	89.3(5)	N1a–Fe1–N3a	89.0(6)
N1a–Fe1–N3c	89.0(6)	N1a–Fe1–N3e	91.0(6)
N3a–Fe1–N3c	89.3(5)	N3a–Fe1–N3e	180.00
N3c–Fe1–N3e	90.7(5)		
173 K			
Fe(1)–N(1)	2.102(12)	Fe(1)–N(1d)	2.102(12)
Fe(1)–N(4)	2.200(8)	Fe(1)–N(4d)	2.200(8)
Fe(1)–N(2a)	2.096(12)	Fe(1)–N(2e)	2.096(13)
N1–Fe1–N4	89.4(4)	N1–Fe1–N2a	91.4(5)
N1–Fe1–N1d	180.00	N1–Fe1–N4d	90.6(4)
N1–Fe1–N2e	88.6(5)	N2a–Fe1–N4	89.7(4)
N1d–Fe1–N4	90.6(4)	N4–Fe1–N4d	180.00
N1d–Fe1–N2a	88.6(5)	N2a–Fe1–N4d	90.3(4)
N2e–Fe1–N4	90.3(4)	N2a–Fe1–N2e	180.00
N1d–Fe1–N4d	89.4(4)	N1d–Fe1–N2e	91.4(5)
N2e–Fe1–N4d	89.7(4)		
194 K			
Fe1–N1	1.996(18)	Fe1–N3	1.942(9)
Fe1–N1a	1.996(18)	Fe1–N3a	1.942(9)
Fe1–N3c	1.942(9)	Fe1–N3e	1.942(9)
N1–Fe1–N3	90.1(5)	N1–Fe1–N1a	180.00
N1–Fe1–N3a	89.9(5)	N1–Fe1–N3c	89.9(5)
N1–Fe1–N3e	90.1(5)	N1a–Fe1–N3	89.9(5)
N3–Fe1–N3a	89.9(4)	N3–Fe1–N3c	180.00
N3–Fe1–N3e	90.1(4)	N1a–Fe1–N3a	90.1(5)
N1a–Fe1–N3c	90.1(5)	N1a–Fe1–N3e	89.9(5)
N3a–Fe1–N3c	90.1(4)	N3a–Fe1–N3e	180.00
N3c–Fe1–N3e	89.9(4)		
273 K			
Fe1–N3	2.147(6)	Fe1–N1	2.226(5)
Fe1–N4a	2.145(6)	Fe1–N3c	2.147(6)
Fe1–N1c	2.226(5)	Fe1–N4d	2.145(6)

N3–Fe1–N1	88.7(2)	N3–Fe1–N4a	88.9(2)
N3–Fe1–N3c	180.00	N3–Fe1–N1c	91.3(2)
N3–Fe1–N4d	91.1(2)	N1–Fe1–N4a	88.2(2)
N3c–Fe1–N1	91.3(2)	N1–Fe1–N1c	180.00
N1–Fe1–N4d	91.8(2)	N3c–Fe1–N4a	91.1(2)
N1c–Fe1–N4a	91.8(2)	N4a–Fe1–N4d	180.00
N3c–Fe1–N1c	88.7(2)	N3c–Fe1–N4d	88.9(2)
N1c–Fe1–N4d	88.2(2)		